Optical parametric master oscillator and power amplifier for efficient conversion of high-energy pulses with high beam quality

Gunnar Arisholm, Ørnulf Nordseth, and Gunnar Rustad

FFI (Norwegian Defence Research Establishment), Postboks 25, NO-2027 Kjeller, Norway

gunnar.arisholm@ffi.no

Abstract: We describe a system for parametric conversion of high-energy, Q-switched laser pulses from 1.064 μm to 2.1 μm in $KTiOPO_4$. High beam quality and efficiency are obtained by use of a two-stage system: An optical parametric oscillator (OPO) pumped by a narrow beam with 8 mJ of energy, generates 1.9 mJ of signal energy for seeding an optical parametric amplifier (OPA). With 500 mJ pump energy, different OPA configurations produce up to 138 mJ signal energy with $M^2 \approx 2.3$.

OCIS codes: (190.4970) Parametric oscillators and amplifiers; (190.4410) Nonlinear optics, parametric processes; (190.2620) Frequency conversion

References and links

1. G.A. Rines, D.M. Rines, and P.F. Moulton, "Efficient, high-energy, KTP optical parametric oscillators pumped with 1 micron Nd-lasers," in *Advanced Solid State Lasers* , T.Y. Fan and B.H.T. Chai, eds., Vol. 20 of OSA Proceedings, (Optical Society of America, Washington DC, 1994), pp. 461-463.
2. M.S. Webb, P.F. Moulton, J.J. Kasinski, R.L. Burnham, G. Loiacono, and R. Stolzenberger, "High-average-power $KTiOAsO_4$ optical parametric oscillator," Opt. Lett. **23**, 1161-1163 (1998).
3. A.V. Smith and M.S. Bowers, "Image-rotating cavity designs for improved beam quality in nanosecond optical parametric oscillators," J. Opt. Soc. Am. B **18**, 706-713 (2001).
4. B.C. Johnson, V.J. Newell, J.B. Clark and E.S. McPhee, "Narrow-bandwidth low-divergence optical parametric oscillator for nonlinear frequency-conversion applications," J. Opt. Soc. Am. B **12**, 2122-2127 (1995).
5. W.A. Neuman and S.P. Velsko, "Effect of cavity design on optical parametric oscillator performance", in *Advanced Solid State Lasers* , S.A. Payne and C.R. Pollock, eds., Vol. 1 of Trends in Optics and Photonics , (Optical Society of America, Washington DC, 1996), pp. 179-181.
6. J.N. Farmer, M.S. Bowers and W.S. Scharpf, "High brightness eyesafe optical parametric oscillator using confocal unstable resonators", in *Advanced Solid State Lasers* , M.M. Fejer and H. Injeyan and U. Keller, eds., Vol. 26 of Trends in Optics and Photonics , (Optical Society of America, Washington DC, 1999), pp. 567-571.
7. S. Haidar and H. Ito, "Injection-seeded optical parametric oscillator for efficient difference frequency generation in mid-IR," Opt. Commun. **171**, 171-176 (1999).
8. Y. Ehrlich, S. Pearl, and S. Fastig, "High brightness tunable tandem optical parametric oscillator at 8-12 μm", in *Advanced Solid State Photonics*, G. Quarles, ed., Vol. 94 of Trends in Optics and Photonics , (Optical Society of America, Washington DC, 2004).
9. D.J. Armstrong and A.V. Smith, "Demonstration of improved beam quality in an image-rotating optical parametric oscillator," Opt. Lett. **27**, 40-42 (2002).
10. A.V. Smith and D.J. Armstrong, "Nanosecond optical parametric oscillator with 90° image rotation: design and performance," J. Opt. Soc. Am. B **19**, 1801-1814 (2002).
11. G.T. Moore and K. Koch, "Efficient high-gain two-crystal optical parametric oscillator," IEEE J. Quantum Electron. **31**, 761-768 (1995).
12. W.R. Bosenberg and D.R. Guyer, "Broadly tunable, single-frequency optical parametric frequency-conversion system," J. Opt. Soc. Am. B **10**, 1716-1722 (1993).

#4787 - $15.00 US Received 12 July 2004; revised 18 August 2004; accepted 18 August 2004

13. J.C. McCarthy, R.C. Day, and E. Chicklis, "Novel, efficient, high brightness KTP optical parametric oscillator-amplifier in single beamline," in *Advanced Solid State Lasers* , C. Marshall, ed., Vol. 50 of Trends in Optics and Photonics , (Optical Society of America, Washington DC, 2001), pp. 656-659.
14. R.W. Boyd, *Nonlinear optics*, (Academic Press, San Diego, 1992).
15. S.J. Brosnan and R.L. Byer, "Optical parametric oscillator threshold and linewidth studies," IEEE J. Quantum Electron. **15**, 415-431 (1979).
16. B.C. Stuart, M.D. Feit, S. Herman, A.M. Rubenchik, B.W. Shore, and M.D. Perry, "Nanosecond-to-femtosecond laser-induced breakdown in dielectrics," Phys. Rev. B **53**, 1749-1761 (1996).
17. M. Missey, V. Dominic, and P.E. Powers, "Periodically poled lithium niobate monolithic nanosecond optical parametric oscillators and generators," Opt. Lett. **24**, 1227-1229 (1999).
18. G. Arisholm, R. Paschotta, and T. Sdmeyer, "Limits to the power scalability of high-gain optical parametric amplifiers," J. Opt. Soc. Am. B **21**, 578-590 (2004).
19. A. Fragemann, V. Pasiskevicius, G. Karlsson, and F. Laurell, "High-peak power nanosecond optical parametric amplifier with periodically poled KTP," Opt. Express **11**, 1297-1302 (2003).
20. W.A. Neuman, "OPO performance with an aberreated input pump beam," in *Nonlinear frequency generation and conversion*, M.C. Gupta, W.J. Kozlovsky, and D.C. MacPherson, eds., Proc. SPIE **2700**, 250-261 (1996).
21. L.R. Marshall, A. Kaz, and O. Aytur, "Multimode pumping of optical parametric oscillators," IEEE J. Quantum Electron. **32**, 177-182 (1996).
22. International Organization for Standardization, "Lasers and laser-related equipment – Test methods for laser beam parameters – Beam widths, divergence angle and beam propagation factor," ISO 11146, (Geneva, 1999).

1. Introduction

Optical parametric oscillators (OPOs) can be useful in a number of applications such as spectroscopy, military countermeasures, and remote sensing. In all these applications, high pulse energy may be required. OPOs have been scaled to several hundred millijoules [1, 2], but combining high energy, high efficiency and good beam quality in nanosecond OPOs is known to be difficult [3]. A fundamental problem with efficiency in pulsed OPOs is the build-up time of the resonant wave(s). The leading part of the pump pulse provides gain for the signal to grow from quantum noise, but the pump is not efficiently converted until the signal power has grown comparable to the pump. Thus, high efficiency is only possible if the build-up time is short compared to the duration of the pump pulse, and this condition is more difficult to achieve for short pump pulses. This problem is not limited to high-energy OPOs, but it is particularly relevant in that context because many high-energy lasers generate pulses only a few nanoseconds long.

The second problem, which is specific to high-energy OPOs, is that the beam diameter must be increased to scale an OPO to higher energy without exceeding the damage threshold of nonlinear crystals and other optics. The resonator length, on the other hand, must remain small to keep the build-up time short. This leads to a resonator with a high Fresnel-number that can support many transverse modes.

Third, backconversion, i.e. that sum frequency generation of signal and idler transfers energy back to the pump wavelength, can reduce both efficiency and beam quality. Backconversion increases with higher intensities or longer crystals, so there is a trade-off between high gain and low backconversion. The shorter the pump pulse is, the higher gain is required to keep the build-up time short, and therefore backconversion is especially pronounced in high-energy, short-pulsed OPOs.

The problem with transverse mode control has been addressed by use of confocal unstable resonators [4–8], where the magnification reduces the divergence. This type of resonator has the useful property that the beam is well collimated in the forward direction, but the large divergence in the return pass limits the efficiency of two-pass pumping in critically phase-matched crystals, making it more difficult to achieve a short build-up time. Another method to reduce the divergence is to exploit the limited acceptance angle in a type 2 critically phase-matched interaction. This effect usually leads to an asymmetric beam with small divergence only in the critical plane, but by image rotating the beam this effect can give good beam quality

#4787 - $15.00 US Received 12 July 2004; revised 18 August 2004; accepted 18 August 2004

in both directions [3, 9, 10]. A disadvantage is that the optics for image rotation can increase the build-up time by making the cavity longer.

Backconversion can create severe beam distortions in a single pass through the nonlinear crystal, so this problem is not eliminated by unstable resonators or image rotation. High gain and low backconversion can be combined by use of multiple gain passes with idler output coupling between them. A ring resonator with multiple crystals allows the crystal length for each gain pass to be individually optimized [11], but a two-pass pumped linear resonator with idler output in both ends is simpler and exploits the same principle. As mentioned above, an unstable resonator is not ideal for two-pass pumping, and the more general multi-crystal ring resonator tends to make the round trip time longer. The image rotating ring cavity lends itself to multiple crystals, but the image rotation also affects the polarization, and simultaneous polarization control at the pump and signal wavelengths is difficult to implement.

A two-stage system consisting of a master oscillator and a power amplifier (MOPA), where the master oscillator is an OPO and the power amplifier is an OPA, can address all three problems. First, although the build-up time of the oscillator is still an issue, the OPA pump can be delayed to overlap the signal pulse optimally. Thus, even if the signal pulse is significantly shorter than the pump pulse, one can at least arrange that the peak of the pump pulse, rather than its tail, is converted efficiently. Second, the output energy and efficiency of the whole system are essentially determined by the OPA, so the master OPO can operated with a narrow, low-energy pump beam to suppress higher order transverse modes. The signal beam is expanded and fed into the power OPA together with a large-diameter pump beam containing most of the available pump energy. If the input signal is strong enough to dominate the noise, the large beam diameter in the OPA does not cause multiple transverse modes to grow. Third, although backconversion can occur in the OPA, it is easier to control. The gain of the OPA can be chosen with respect to only output energy and backconversion, whereas the gain in a single OPO must be high to minimize the build-up time. The technique with idler output coupling between amplifier stages, as in OPOs with multiple gain passes, is even more advantageous in an OPA because it is less important to keep the optical path short, and the loss associated with additional mirrors is less critical outside the cavity.

Parametric MOPAs have been reported before. One system [12] produced single-frequency radiation over a very wide tuning range, but the OPA had only modest efficiency. Another system [13] had a simple structure with a single beam line, but that design does not offer the freedom to optimize the temporal overlap between the pump and seed pulses to the OPA or to expand the signal beam before the OPA. A related approach, which has been used to improve the spectral purity of OPOs, is the master oscillator and power oscillator (MOPO) configuration [4, 7, 12], in which a low-energy master OPO provides a seed signal to a power OPO.

The topic of this paper is to demonstrate scaling of a parametric MOPA to the 250 mJ output energy level. Section 2 presents some background theory. Section 3 describes the experimental setup for conversion from $1.064\,\mu$m to $2.1\,\mu$m, and we present the experimental results in Section 4. Conclusions are drawn in Section 5.

2. Scaling properties of OPOs and OPAs

In this section we discuss some properties of OPOs and OPAs related to scaling to short pulses and large beam diameters. For the general theory of OPOs and OPAs we refer to the literature, e.g. Refs. [14, 15]. We number the idler, signal and pump beams 1, 2, and 3, respectively, and denote their angular frequencies by ω_j and their refractive indices in the nonlinear crystal by n_j.

Consider first scaling of the pulse length in an OPO. The ratio of the build-up time to the

#4787 - $15.00 US Received 12 July 2004; revised 18 August 2004; accepted 18 August 2004

pump pulse length can be estimated by a simple calculation for plane waves and a rectangular pump pulse of duration t_p. The gain coefficient is $g = \kappa I_3^{1/2}$, where I_3 is the pump intensity, $\kappa = (\omega_1\omega_2)^{1/2}\gamma$, $\gamma = 2d_{\text{eff}}(2n_1n_2n_3c^3\varepsilon_0)^{-1/2}$, d_{eff} is the effective nonlinear coefficient, ε_0 is the vacuum permittivity, and c is the speed of light in vacuum. The maximum I_3 is limited by the damage threshold of the material. The fluence damage threshold in the nanosecond regime scales approximately as $t_p^{1/2}$ [16], so we take $I_3 \propto t_p^{-1/2}$ and obtain $g \propto t_p^{-1/4}$. We assume that the OPO operates in the high-gain regime so that the single-pass amplitude gain $\cosh(gL_c) \approx \exp(gL_c)/2$, where L_c is the length of the crystal.

Let $\exp(G)$ be the total amplitude gain required to amplify the initial noise to a level sufficient to deplete the pump. Then the required number N of round trips for the signal to build up is determined by $G \approx N(L_c g - \ln(2) + \ln(R)/2)$, where R denotes the effective reflectivity of the output coupler, i.e. the total round-trip loss of the cavity is $1-R$. The build-up time is $t_b \approx Nt_r$, where t_r is the cavity round trip time. If the air gaps are short so that the crystal accounts for most of the round trip time, $t_r \approx 2L_c n/c$. Combining these equations, we obtain

$$t_b \approx \frac{2GL_c n}{(L_c g + \ln(R)/2 - \ln(2))c}. \tag{1}$$

If $L_c g$ is sufficiently large to dominate the denominator, $t_b \approx 2Gn/(cg)$, which is independent of L_c because a longer crystal not only increases the gain but also the round trip time. Hence, $t_b \propto g^{-1} \propto t_p^{1/4}$, and the ratio $t_b/t_p \propto t_p^{-3/4}$ increases for short pulses. As a numerical example, consider a crystal with $d_{\text{eff}} = 2\,\text{pm/V}$, $n_j \approx 1.7$, $I_{3,\max} = 600\,\text{MW/cm}^2$ for $t_p = 5\,\text{ns}$ pulses, and take $G \approx 18$. These values are representative for an OPO based on $KTiOPO_4$ (KTP). For $\lambda_3 = 1\,\mu\text{m}$, $\lambda_1 = \lambda_2 = 2\,\mu\text{m}$, $L_c = 20\,\text{mm}$, and $R = 0.5$ we obtain $t_b = 1.7\,\text{ns}$ from Eq. (1). For $t_p = 20\,\text{ns}$, $I_{3,\max}$ would scale to 300 MW/cm^2, and t_b would only increase to 2.5 ns. For short pump pulses, optical parametric generators (OPGs) can be more suitable than OPOs. Because the OPG is a single-pass device, its performance depends essentially on the peak intensity, which scales favourably for shorter pusles. The performance of OPOs and OPGs for pulses in the few nanosecond range has been compared in Ref. [17].

Consider now scaling of the transverse beam size. Although the beam quality of an OPO can be improved by an unstable resonator, this method does not allow scaling to arbitrary beam diameter. A high quality beam is only established after a small patch near the centre has been magnified to cover the whole mode, and this takes more round trips for a beam with large diameter. A similar argument holds for the image rotating cavity, where the spatially coherent zone of the beam is expanded by transverse walk-off. An OPA, on the other hand, can in principle be scaled to arbitrary beam diameter. However, a nonuniform pump intensity leads to tranversely varying gain, and this can limit efficiency and beam quality. For narrow beams, diffraction can redistribute signal power across the beam and give good beam quality and efficiency even with very high gain [18], but this is not the regime of interest for high-energy pulses. When the beam diameters are large and the gain is high, the intense parts of the pump beam will be depleted before the low intensity parts are efficiently converted. Increasing the gain to improve conversion in the low-intensity parts leads to backconversion in the high-intensity parts. This problem can be reduced by coupling out the idler between multiple stages, as mentioned above, and also by expanding the signal beam between the stages [18, 19]. Thus, by suitable measures to control beam diameter and backconversion, an OPA can be scaled to large beam diameter without sacrificing efficiency or beam quality.

Temporal variation of the pump pulse to the OPA can also lead to a trade-off between efficient conversion of the low-intensity parts and backconversion in the peaks. A smooth single-frequency pulse is preferrable to a multi-longitudinal-mode (MLM) pulse, but this problem can also be reduced by idler output coupling between the stages.

#4787 - $15.00 US Received 12 July 2004; revised 18 August 2004; accepted 18 August 2004

Finally, it should be noted that phase front aberrations of the pump beam to an OPA or singly resonant OPO need not be tranferred to the signal because the idler phase can adapt to cancel them. However, the intensity variations that are usually present in a low-quality pump beam lead to spatial variation of the gain, which does reduce the quality of the signal beam. Experiments and simulations of OPOs pumped by multi-mode beams [20, 21] indicate that the beam quality of the signal deteriorates and can become worse than the quality of the pump beam.

3. Experimental set-up

Figure 1 shows the OPO and the OPA. The pump laser (not shown) is a Quantel Brilliant B, delivering 1.064 μm pulses of about 650 mJ (after a polarizer to clean up depolarization caused by thermal stress) at 10 Hz repetition rate. The pulse length is about 6 ns (FWHM), and the laser operates on multiple longitudinal modes. By using a silicon CCD camera to measure the beam diameter at various positions near a waist and a few Rayleigh lengths away from it, we estimated the beam quality to be $M^2 \approx 2$. The master oscillator has a single 20 mm long KTP crystal cut with $\theta \approx 50.5^\circ$ for type 2 (oeo) phase matching. It was tuned to operate with the signal at $\lambda_2 = 2.08\,\mu$m and idler at $\lambda_1 = 2.18\,\mu$m. The input mirror (M1) has transmission $T \approx 0.99$ for the pump, reflection $R > 0.99$ for the signal, and $R \approx 0.5$ for the idler. The output coupler (M2), designed for two-pass pumping, has $R > 0.99$ for the pump, $R \approx 0.77$ for the signal, and $T \approx 0.95$ for the idler. The total round trip signal loss from the AR coatings and the HR mirror is about 2%. The gaps between the crystal and the mirrors are 1–2 mm. A telescope images and demagnifies the pump beam from the laser to the OPO. The object plane of the telescope was chosen inside the laser to obtain a relatively flat-topped pump fluence distribution. The resulting pump beam has a diameter of about 1.1 mm (90% encircled energy). After the OPO there are two 45° mirrors (M3, M4) to remove the idler and any transmitted pump. M4 also combines the signal with the pump beam to the OPA. A telescope (L1, L2) expands the signal beam by a factor 8 to make its diameter somewhat greater than that ofthe OPA pump beam. This expansion also acts as a spatial filter because only the central part of the signal beam overlaps with the pump beam in the OPA.

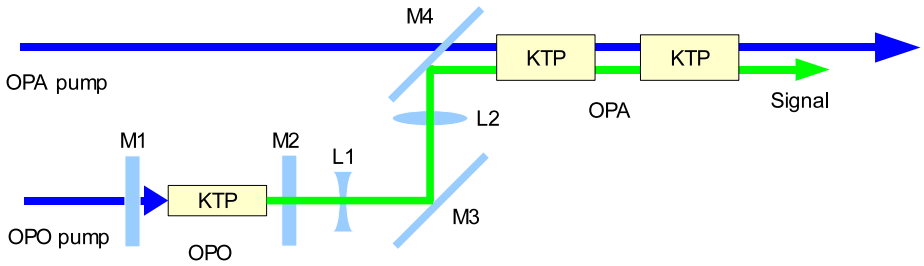

Fig. 1. Experimental layout of the OPO and the OPA. The number of crystals in the OPA was varied between 2 and 4, and idler filters could be inserted between some of the crystals.

The OPA consists of 2–4 KTP crystals oriented for walk-off compensation. Each crystal is 15 mm long and cut at the same angle as the oscillator crystal. The OPA pump beam is also relay imaged from the laser, but with a greater magnification, and the intermediate focus of the telescope is located in an evacuated tube to avoid breakdown in the air. The resulting beam at the OPA is slightly elliptic, with diameters of 6.5 mm by 5.4 mm. The pump path from the laser to the OPA is about 80 cm longer than the path through the OPO to compensate for the build-up time of the OPO and optimize the relative timing of the pulses input to the OPA. Filter mirrors at 45°, highly reflective for pump and signal and highly transmitting for the idler, could

#4787 - $15.00 US
Received 12 July 2004; revised 18 August 2004; accepted 18 August 2004

be inserted between crystals 2 and 3 or between crystals 3 and 4 to reduce backconversion in the final crystals. The beams output from the OPA were separated by filter mirrors and diagnosed by a pyroelectric camera (Spiricon Pyrocam-1), power meters (Ophir with 10A-P head), and a scanning knife edge.

4. Results

Figure 2 shows the output signal energy from the OPO as function of the input pump energy. The maximum conversion efficiency to signal is 24 %. For signal beam characterization we formed a waist with an $f = 200\,\mathrm{mm}$ lens and obtained the corresponding far field with a second $f = 250\,\mathrm{mm}$ lens. Figure 3 shows the fluence distributions. The minimum width for the critical and noncritical directions occured at approximately the same position, so only one picture is shown for the waist.

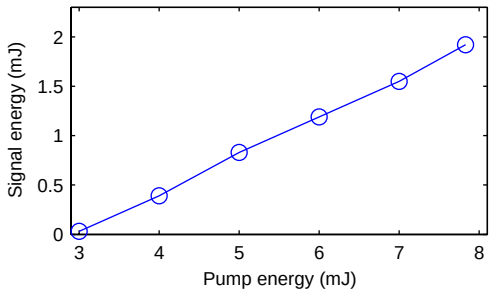

Fig. 2. Signal energy vs. pump energy for the OPO.

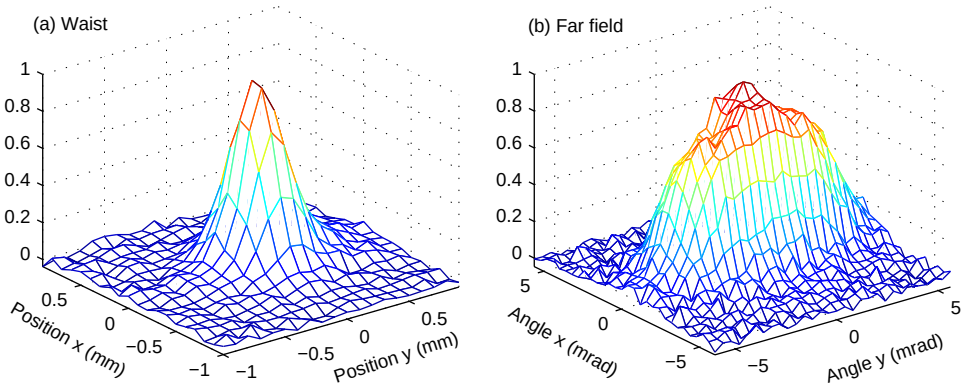

Fig. 3. Signal beam of the OPO after an $f = 200\,\mathrm{mm}$ lens, measured with the pyroelectric camera. The pump energy was 8 mJ. (a) Waist. (b) Far field (after the lens, not directly from the OPO). The x and y coordinates correspond to the critical and noncritical directions, respectively. All fluence data have been normalized to unity peak value.

The pyroelectric camera is too noisy for reliable calculation of beam parameters, so we measured the beam widths independently with a scanning knife edge and estimated the M^2 beam quality from the 16–84% knife-edge widths with the method from Ref. [22]. The results, $M_x^2 \approx 1.6$ for the critical direction and $M_y^2 \approx 3.4$ for the noncritical direction, confirm

#4787 - $15.00 US
Received 12 July 2004; revised 18 August 2004; accepted 18 August 2004

the expectation that the small acceptance angle in the critical direction reduces divergence and improves beam quality. Table 1 shows the beam parameters for the OPO and various OPA configurations. The waist diameters, d_x and d_y, are defined to be two times the 16–84% knife-edge width, so that they equal the $\exp(-2)$ diameter for a Gaussian beam. The divergence angles, θ_x and θ_y, are defined analogously, so the product $d \times \theta$ would be $4\lambda/\pi = 2.65\,\mathrm{mm}\times\mathrm{mrad}$ for a Gaussian beam with $\lambda = 2.08\,\mu\mathrm{m}$. We emphasize that only the products $d \times \theta$ represent real measurements, the M^2 values are estimates that are not based on the true second moments. Also note that the estimation of M^2 from the product $d \times \theta$ includes a correction factor [22], it is not simply a division by the value for a Gaussian beam. The accuracy of the estimate depends on the beam, in particular, the knife-edge method may give an optimistic value for an energy distribution with a small pedestal [9].

All the OPA measurements were performed with the OPO operating at 8 mJ pump energy, yielding 1.9 mJ signal output from the OPO, and 0.9 mJ seed energy inside the aperture of the OPA crystals. Figure 4 shows the output signal energy as function of OPA pump energy. The approximately linear shape of the curves even in the regime of small conversion differs from the exponential shape that might be expected theoretically. The reason is that an MLM pump pulse contains a wide range of intensities, with the highest spikes reaching saturation even at relatively low energy. Simulations with a single-frequency pump showed the expected shape, and with an MLM pump they reproduced the nearly linear curve from the experiments. We do not know the exact damage threshold of the AR coatings on the crystals, but for safety we limited the pump energy to 500 mJ to keep the peak fluence below 3 J/cm^2.

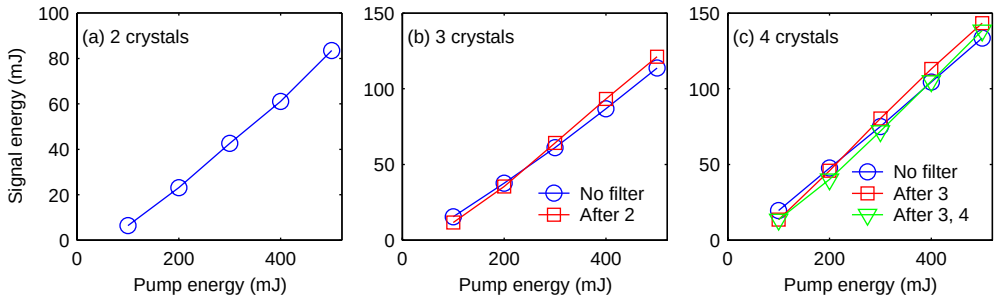

Fig. 4. Signal energy vs. pump energy for OPAs with 2, 3, or 4 crystals. The red and green curves correspond to the OPAs with idler filters after certain crystals, as shown in the legends.

Measurements on the two-crystal OPA showed that it was not very sensitive to the seed energy, for example, a reduction of the seed by 50% reduced the output energy by $< 15\%$. The sensitivity to seed energy should be even lower with more crystals, but we did not measure this for all configurations.

The OPA signal beam was characterized by the same method as the beam from the OPO, using an $f = 500\,\mathrm{mm}$ lens to form a waist and an $f = 250\,\mathrm{mm}$ lens to obtain the far field. The beam parameters are summarized in Table 1. For the two-crystal OPA, M_y^2 is better than from the OPO alone, and this can be explained by the spatial filtering induced by expansion of the seed beam. The quality of the idler beam is somewhat worse than the signal. This was expected because when the signal beam wavefront is constrained by the seed beam, the idler wavefront adapts to aberrations in the pump beam. The idler beam was not characterized for the other configurations.

The strongly reduced beam quality for the OPAs with 3 or 4 crystals can be ascribed to pump depletion and subsequent backconversion, which affects both the intensity and the wavefront of

#4787 - $15.00 US
Received 12 July 2004; revised 18 August 2004; accepted 18 August 2004

the signal beam. Most of the OPAs have better beam quality in the critical than in the noncritical direction, for the same reason as for the OPO. The exception for the OPA with three crystals is probably due to the uncompensated walk-off of the signal beam in the odd number of crystals.

The backconversion can be reduced by coupling the idler beam out between some of the OPA crystals, at the cost of splitting the total idler energy among multiple beams. For the 3-crystal OPA with idler filter after crystal 2 and for the 4-crystal OPA with idler filters after crystals 2 and 3 this technique leads to substantially improved beam quality and slightly higher signal energy, as shown in the table. In both these configurations, 80 mJ of idler energy in a single beam with $M^2 \approx 2.7$ is still available after crystal 2. Figure 5 shows the measured fluence distributions for the 4-crystal OPA with two idler filters. Idler filtering only after crystal 3 in the 4-crystal OPA gave the highest signal energy, but the beam quality did not improve much because it was already poor after crystal 3.

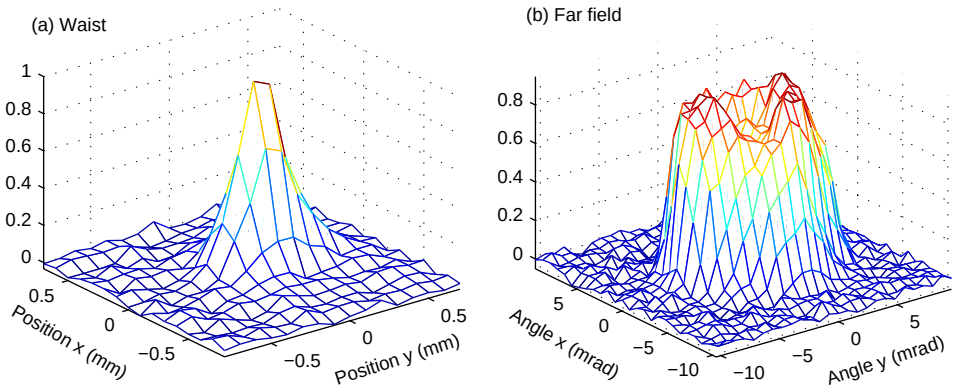

Fig. 5. Waist (a) and far-field (b) measured after an $f = 500\,\mathrm{mm}$ lens in the signal beam from the 4-crystal OPO with idler filters after crystals 2 and 3. The pump energy was 500 mJ.

Table 1. Beam parameters for the signal from the OPO and various OPA configurations, and for the idler from the two-crystal OPA. All the OPAs were pumped by 500 mJ. The numbers in the OPA configurations indicate the number of crystals, and the suffixes B or C indicate configurations with idler output coupling. The widths d and θ are two times the 16%–84% knife-edge width, and the x and y coordinates correspond to the critical and noncritical directions, respectively. M^2 is an estimate of the overall beam quality, based on the RMS values of the x and y widths. The last column shows the signal (or idler) energy.

	Idler filter after crys.	$d_x\theta_x$ mm×mrad	$d_y\theta_y$ mm×mrad	M_x^2	M_y^2	M^2	Energy mJ
OPO		4.75	11.1	1.6	3.4	2.6	1.9
OPA 2		5.56	7.60	1.9	2.4	2.2	84
OPA 3		12.5	12.0	3.8	3.7	3.8	114
OPA 4		13.7	17.7	4.1	5.2	4.7	133
OPA 3B	2	5.25	8.84	1.8	2.8	2.3	121
OPA 4B	3	13.5	16.9	4.1	5.0	4.5	143
OPA 4C	2, 3	6.37	8.18	2.1	2.6	2.3	138
OPA 2, idler		8.05	9.30	2.5	2.8	2.7	80

#4787 - $15.00 US
Received 12 July 2004; revised 18 August 2004; accepted 18 August 2004

5. Conclusions

A parametric master oscillator / power amplifier system has demonstrated conversion of 500 mJ, 6 ns pulses with high efficiency and beam quality. The optimal configuration depends on the application of the idler beam. If it is important to have all the idler energy in a single beam, an OPA without intermediate idler output coupling must be used. In this case there is a strong trade-off between output energy and beam quality, with total conversion efficiency (signal + idler) of 33%, 45%, or 52% and signal M^2 of 2.2, 3.8, or 4.7 for OPAs with 2, 3, or 4 crystals, respectively. If multiple idler beams are acceptable, 28% conversion to signal can be obtained with $M^2 \approx 2.4$. These efficiencies and beam qualities compare favourably with other reported results for high-energy parametric frequency conversion [1, 2, 4–8].

The main disadvantage of the MOPA compared to a single OPO is the complexity of two separate pump beam paths. In a tunable system, the need to adjust the angle (or other parameters) of multiple crystals also increases complexity, but even a single-stage OPO might well need two crystals for walk-off compensation. To conclude, although the MOPA is more complex than a single-stage OPO, it offers more flexibility for transverse mode control, suppression of backconversion, operation with even shorter pulses, and further scaling of the energy.

Acknowledgments

We thank Knut Stenersen for helpful suggestions.

#4787 - $15.00 US Received 12 July 2004; revised 18 August 2004; accepted 18 August 2004